IOP Conf. Series: Journal of Physics: Conf. Series **1023** (2018) 012024 doi:10.1088/1742-6596/1023/1/012024

# Signatures for a nuclear quantum phase transition from $E0$ and $E2$ observables in Gd isotopes

**J. Wiederhold[1], R. Kern[1], C. Lizarazo[1], N. Pietralla[1], V. Werner[1], R.V. Jolos[2,3], D. Bucurescu[4], N. Florea[4], D. Ghita[4], T. Glodariu[4], R. Lica[4], N. Marginean[4], R. Marginean[4], C. Mihai[4], R. Mihai[4], I.O. Mitu[4], A. Negret[4], C. Nita[4], A. Olacel[4], S. Pascu[4], L. Stroe[4], S. Toma[4], A. Turturica[4]**

[1] Institut für Kernphysik, Technische Universität Darmstadt, Schlossgartenstr. 9, 64289 Darmstadt, Germany
[2] Joint Institute for Nuclear Research, Dubna, Moscow oblast, 141980 Russia
[3] Dubna State University, Dubna, Moscow oblast, 141980 Russia
[4] "Horia Hulubei" National Institute for Physics and Nuclear Engineering, 077125, Bucharest-Magurele, Romania

E-mail: jwiederhold@ikp.tu-darmstadt.de

**Abstract.** Nuclei are complex quantum objects due to complex nucleon-nucleon interactions. They can undergo rather rapid changes in structure as a function of nucleon number. A well known region of such a shape transition is the rare-earth region around $N = 90$, where accessible nuclei range from spherical nuclei at the closed neutron shell at $N = 82$ to deformed nuclei. For a better understanding of this phenomenon, it is of interest to study empirical signatures like the $E2$ transition strength $B(E2; 2_1^+ \rightarrow 0_1^+)$ or the $E0$ excitation strength $\rho^2(E0; 0_1^+ \rightarrow 0_2^+)$. The nuclide $^{152}$Gd with 88 neutrons is located close to the quantum phase transition at $N = 90$. The lifetime $\tau(0_2^+)$ of $^{152}$Gd has been measured using fast electronic scintillation timing (FEST) with an array of HPGe- and $LaBr_3$- detectors. Excited states of $^{152}$Gd were populated via an ($\alpha$,n)-reaction on a gold-backed $^{149}$Sm target. The measured lifetime of $\tau(0_2^+) = 96(6)$ ps corresponds to a reduced transition strength of $B(E2; 0_2^+ \rightarrow 2_1^+) = 111(7)$ W.u. and an $E0$ transition strength of $\rho^2(E0) = 39(3) \cdot 10^{-3}$ to the ground state. This result provides experimental support for the validity of a correlation between $E0$ and $E2$ strengths that is a novel indicator for a quantum phase transition. This work was published as J. Wiederhold *et al.*, Phys. Rev. C **94**, 044302 (2016).

## 1. Introduction

The rare-earth region around the neutron number $N = 90$ is a well known region where nuclei can undergo a quantum shape phase transition (QPT) [1, 2, 3], a rather rapid change of structure as a function of neutron number. Well known empirical signatures of a shape change in a sequence of even-even nuclei are, e.g., a sudden change in the energy ratio $R_{4/2}$ of the $2_1^+$ and $4_1^+$ level energies $E(4_1^+)$ and $E(2_1^+)$ or a change in the easier to obtain inverse of the energy $E(2_1^+)$, a sharp change of the $E2$-transition strength connecting the ground state to the first-excited $2_1^+$ state $B(E2; 0_1^+ \rightarrow 2_1^+)$, the occurrence of a local extreme point of the two-neutron separation energy $S_{2N}$, and a maximum of the $E0$-transition strength $\rho^2(E0)$ at the critical point [4, 5, 6]. Studying the correlation of these observables is essential for the understanding of the phenomenon

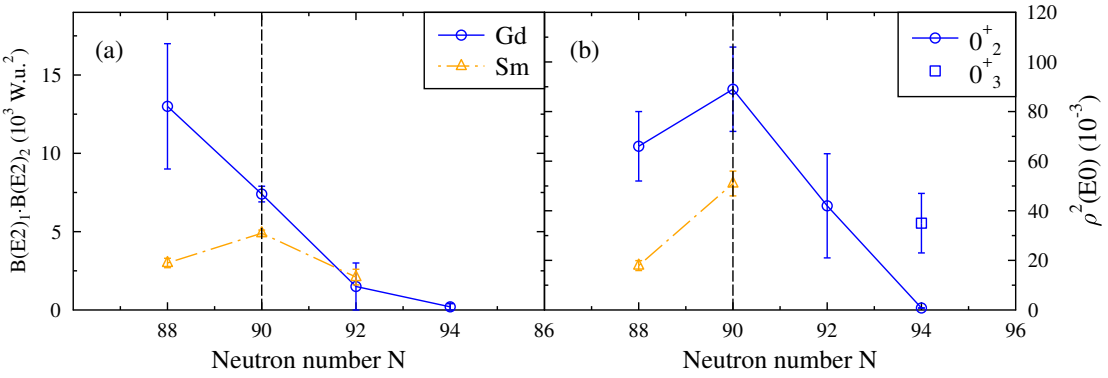


**Figure 1.** (a) Product $B(E2)_1 \cdot B(E2)_2$ (see text) over neutron number for the Gd- (blue) and Sm- (orange) isotopes. (b) The $E0$ transition rate $\rho^2(E0)$ for the Gd- and Sm-isotopes around N=90. For $^{158}$Gd also the $\rho^2(E0; 0_3^+ \rightarrow 0_{gs}^+)$ transition strength is given. Data taken from the Nuclear Data Sheets [7] and [8, 9].

of nuclear shape phase transitions [10, 11, 12].
In a geometrical picture it has been shown [13] that the $E0$-transition strength $\rho^2(E0; 0_2^+ \rightarrow 0_1^+)$ can be connected to a product of $B(E2)$-values. Applying the Q-phonon scheme [14, 15, 16, 17, 18, 19], this results to:

$$\rho^2(E0) \approx \left(\frac{4\pi}{3Z}\right)^2 \frac{5}{(eR^2)^4} B(E2)_2 B(E2)_1, \tag{1}$$

with the proton number $Z$, the radius $R$ of the atomic nucleus, $B(E2)_1 = B(E2; 2_1^+ \rightarrow 0_1^+)$ and $B(E2)_2 = B(E2; 0_2^+ \rightarrow 2_1^+)$. The left-hand side of Figure 1 shows the available data for the product of $B(E2)$-values, while on the right-hand side the available $\rho^2(E0; 0_2^+ \rightarrow 0_1^+)$-data of the Gd- and Sm-isotopes around $N = 90$ are depicted. The available data partly supports the relation of Equation (1). Both, the $\rho^2(E0; 0_2^+ \rightarrow 0_1^+)$ and the product of $B(E2)$-values, decrease beyond $N = 90$ and the $\rho^2(E0; 0_2^+ \rightarrow 0_1^+)$ maximizes for both isotopic chains at $N = 90$. Moreover, the product of $B(E2)$-values maximizes at $N = 90$ for the Sm-chain. But, in the case of $^{152}$Gd the correlation seems to be invalid. The value of the product of $B(E2)$-values seems to increase, not decrease, towards $^{152}$Gd with $N = 88$ with an extraordinarily large $B(E2; 0_2^+ \rightarrow 2_1^+)$ value of 178(54) W.u. in this vibrational nucleus, however, with a large uncertainty. The lifetime of the second $0^+$ state of $^{152}$Gd stems mainly from one recoil distance Doppler shift measurement of this lifetime [20]. But the data are dubious. It is in fact mentioned in that work that the statistics for the measurement were not adequate for an accurate lifetime determination by the standard analysis and it was necessary to sum up data from different target-stopper distances. To validate or eventually improve this value a FEST experiment at the 9 MV Tandem accelerator at the National Institute of Physics and Nuclear Engineering (IFIN-HH) in Bucharest has been carried out.

## 2. Experimental setup

An $\alpha$-beam impinging on a 1.3 mg/cm$^2$ thick $^{149}$Sm-target with a 4.3 mg/cm$^2$ gold backing populated excited states of $^{152}$Gd via the $^{149}$Sm($\alpha$,n)$^{152}$Gd fusion-evaporation reaction. The beam energy was set to 17.5 MeV, slightly above the Coulomb barrier for this reaction, to select the one-neutron evaporation channel. The target consisted of 93.2% of $^{149}$Sm and some small

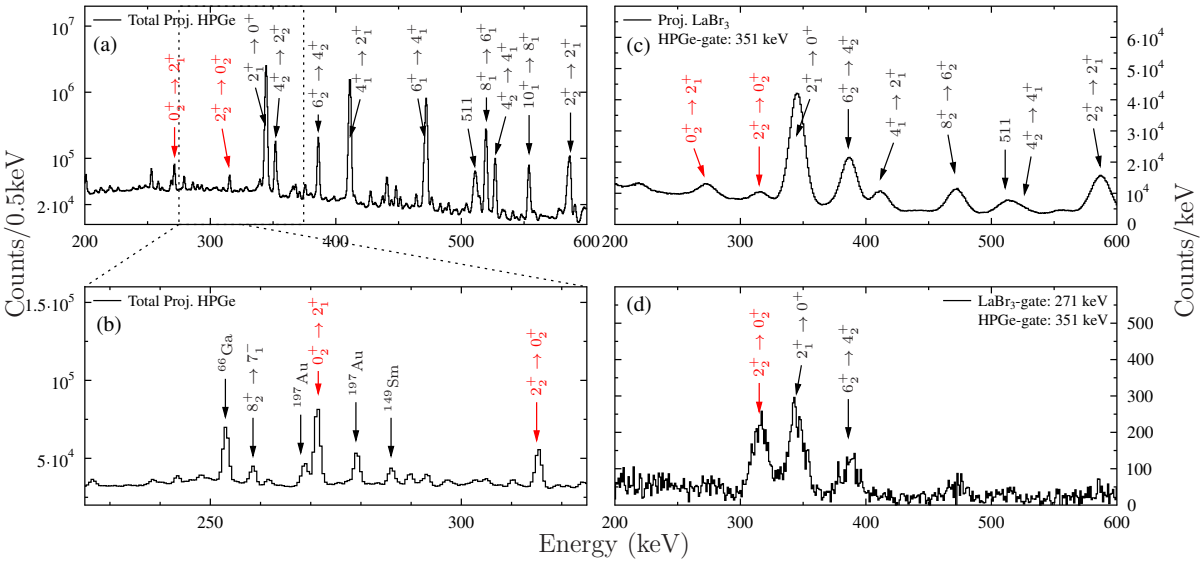


**Figure 2.** (a) Total Projection of the $E_{HPGe}$-$E_{HPGe}$-matrix. (b) Zoomed in on the region of interest between 225 and 325 keV. (c) Energy projection of a $E_{LaBr_3}$-$E_{LaBr_3}$-$\Delta$t-cube in the energy range from 200 to 600 keV. An additional gate was set in the HPGe-detectors on the $4_2^+ \rightarrow 2_2^+$ transition at 351 keV. Marked in red are the important transitions to determine $\tau(0_2^+)$. (d) Coincidence spectrum gated on the 271 keV $0_2^+ \rightarrow 2_1^+$-transition in spectrum (a).

contaminants from other stable Sm-isotopes, i.e. $^{150}$Sm (3.3%), $^{148}$Sm(1.5%), $^{152}$Sm(1.2%), and 0.8% of other elements. The ROSPHERE detector array was used in a configuration of 11 $LaBr_3$- and 14 HPGe-detectors [21] to detect de-excitation $\gamma$-rays of the isotope of interest. The energy calibration and the energy dependent time-walk calibration of the experimental setup were performed using a $^{152}$Eu-source with its well known $\gamma$-ray transitions from $^{152}$Gd and $^{152}$Sm ranging from 244 keV to 1299 keV.

## 3. Analysis and Corrections

### *3.1. Spectroscopy*

Due to the beam energy chosen close to the Coulomb barrier, the reaction channel was clean. The $\gamma$-ray transitions of $^{152}$Gd were clearly identified, by using the HPGe-detectors with an energy resolution of about 3 keV at 1.4 MeV and 2.5 keV at 300 keV. The $\gamma$-ray transitions up to the $10_1^+ \rightarrow 8_1^+$-transition of the yrast band and other bands were identified, including the $\gamma$-transitions necessary to determine the lifetime of the $0_2^+$ state with FEST, i.e. the $2_2^+ \rightarrow 0_2^+$-transition at 315 keV and the $0_2^+ \rightarrow 2_1^+$-transition at 271 keV (See Figure 2). Only a few contaminants from Coulomb excitation of the gold backing of the target and from fusion-evaporation reactions of $\alpha$-particles with Cu parts of the target chamber were found in the energy spectrum. These contaminants were eliminated by setting energy gates in the HPGe-detectors, since they can't be separated from the transitions of interest in the $LaBr_3$-detectors. Figure 2(a) shows the total projection of the HPGe-detector-coincidence matrix between 200 and 600 keV and Figure 2(b) shows the zoomed energy spectra in the energy region 225-325 keV around the relevant transitions for determining the lifetime of the $0_2^+$ state (marked in red). A few small contaminants close to the $0_2^+ \rightarrow 2_1^+$-transition were identified. Figure 2(c) shows the energy projection of the $LaBr_3$-detector-coincidence matrix in coincidence with the 351 keV ($4_2^+ \rightarrow 2_2^+$) transition observed in the HPGe-detectors. After setting an additional gate on the

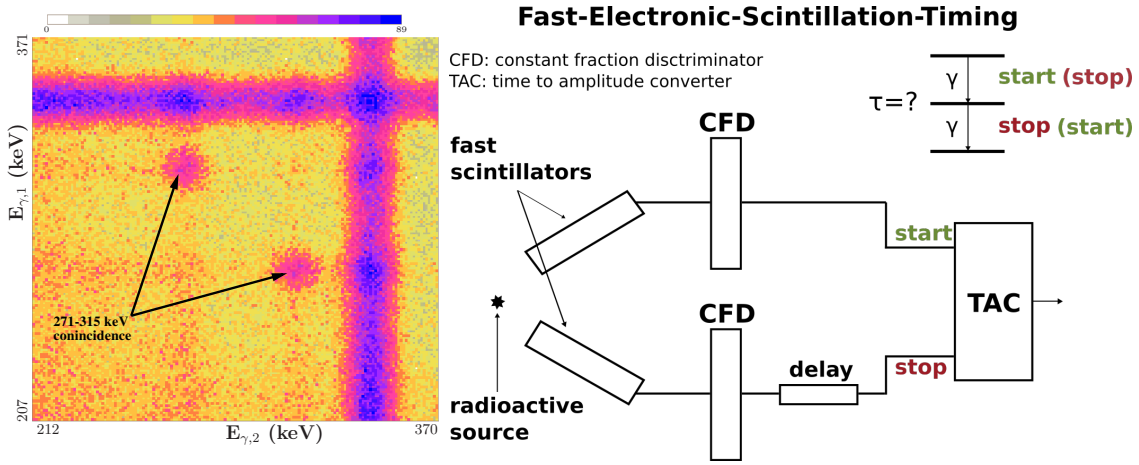


**Figure 3.** (Left) Part of the $E_{\gamma,LaBr_3} - E_{\gamma,LaBr_3}$ matrix obtained after projection of the $E_{\gamma,LaBr_3} - E_{\gamma,LaBr_3} - \Delta t$ cube. Marked are the coincidence areas of the $\gamma$-ray pair 271 and 315 keV, corresponding to the transitions $0_2^+ \rightarrow 2_1^+$ and $2_2^+ \rightarrow 0_2^+$ of $^{152}$Gd. (Right) Simplified FEST setup with two detectors and a source.

$0_2^+ \rightarrow 2_1^+$-transition at 271 keV detected in the $LaBr_3$-detectors, the contaminants in the resulting $LaBr_3$-energy spectra vanish (See Figure 2(d)).

*3.2. Time-Walk*

The lifetime of an excited nuclear state can be determined in a FEST measurement by measuring the time-difference between two signals, e.g. from two $\gamma$-ray transitions. A simplified setup of a FEST measurement is shown in Figure 3 on the right-hand side. These two signals can stem from two $\gamma$-ray transitions, one populating the state of interest and one depopulating it. The measured time-difference is equal to the effective lifetime of the nuclear states between the two $\gamma$-transitions and the energy dependent time-walk of both signals. More details can be found in [22, 23, 24]. Using a $^{152}$Eu-source, a time-walk correction can be applied to the data, as described in [25]. After correcting for the time-walk to measure the lifetimes of excited states, an Energy-Energy-$\Delta t$ cube was sorted for the $LaBr_3$ detectors. By selecting the region of the pair of coincident $\gamma$-rays (e.g. 271 keV and 315 keV for the $0_2^+$ state) in the Energy-Energy plane of this cube (see Figure 3,(left)) a time-difference spectrum can be extracted. A correction for random coincidences and the Compton background was done, by selecting an area near the peak in the Energy-Energy plane. A time-difference spectrum was also established for the surrounding background. It was normalized to the amount of background underneath the coincidence peaks and subtracted from the time-difference spectrum gated on the coincidence peaks. This way, a background-subtracted time difference spectrum for the pair of coincidences was established.
The typical delayed time distribution, assuming no remaining background contributions, is a convolution of the prompt response function (PRF) of the setup, $P(t')$, and the exponential decay [26]:

$$D_\lambda(t) = n\lambda \int_{-\infty}^{t} P(t') e^{-\lambda(t-t')} dt', \tag{2}$$

with the transition rate $\lambda = 1/\tau$ and the normalization $n$.
Depending on the lifetime of the nuclear state of interest, there are different approaches to determine the lifetime, e.g. the slope method [26, 27] or the centroid-shift method [28].
The lifetime of the $0_2^+$ state of $^{152}$Gd was determined with the centroid-shift method [13]. As mentioned above an additional energy gate had to be set in the HPGe-detectors to exclude

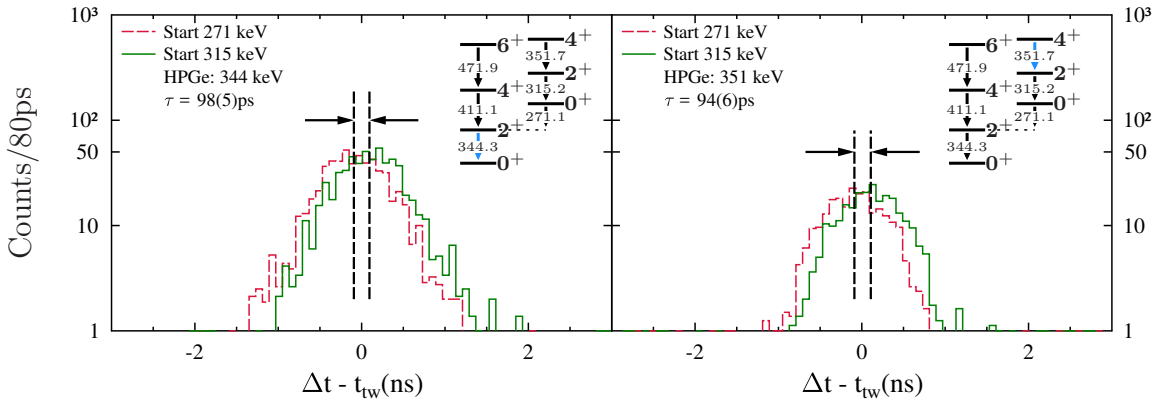


**Figure 4.** (Left) Time-difference-spectra for the combination of start-gate on 315 keV ($2_2^+ \rightarrow 0_2^+$) and stop-gate on 271 keV ($0_2^+ \rightarrow 2_1^+$) in green and vice versa in red (dashed line) with an additional gate on 344 keV ($2_1^+ \rightarrow 0_{gs}^+$) in the HPGe-detectors. (Right) The same with a different gate for the HPGe-detectors ($4_2^+ \rightarrow 2_2^+$ at 351 keV). The right top corner of every time-difference plot shows a partial level scheme of $^{152}$Gd. Marked in blue is the HPGe-gate. The dashed vertical lines mark the centroids of the time-difference spectra. The difference between the centroids is equal to two times the lifetime $\tau(0_2^+)$ of $^{152}$Gd [13].

contributions from any contaminants close to the $0_2^+ \rightarrow 2_1^+$-transition at 271 keV. Figure 4 shows time-difference spectra, one with an additional gate above the state of interest, i.e. the $4_2^+ \rightarrow 2_2^+$-transition at 351 keV (Figure 4,(b)), and one below the $0_2^+$ state on the $2_1^+ \rightarrow 0_{gs}^+$-transition at 344 keV (Figure 4,(a)). Both obtained lifetimes agree within their uncertainties and the lifetime of the $0_2^+$ state of $^{152}$Gd was determined to $\tau = 96(6)$ ps or $T_{1/2} = 67(4)$ ps [13].

## 4. Results and Discussion

From the obtained value for the lifetime $\tau(0_2^+)$ the corresponding $E2$ transition strength with the conversion coefficient $\alpha = 0.0826(12)$ [29] can be calculated to

$$B(E2; 0_2^+ \rightarrow 2_1^+) = 0.536(33)e^2b^2 = 111(7)\text{W.u.} \tag{3}$$

The quoted error represents the statistical uncertainty in determining the centroids and the contributions to the error from the uncertainty of the energy-dependent time-walk. Additionally, a new value for the $\rho^2(E0)$ transition strength can be determined from the $B(E2; 0_2^+ \rightarrow 2_1^+)$-strength using the dimensionless ratio of the $E0$- and $E2$-transitions defined by Rasmussen [30]:

$$X(E0/E2) \equiv \frac{B(E0)}{B(E2)} = \frac{\rho^2(E0)e^2R^4}{B(E2)}. \tag{4}$$

With the literature value of $X(E0/E2) = 0.0122(5)$ [9] one obtains the fairly large value of

$$\rho^2(E0) = 39(3) \cdot 10^{-3}. \tag{5}$$

Figure 5 shows the $\rho^2(E0)$-strength and the product $B(E2)_1 \cdot B(E2)_2$ as a function of the neutron number for the Sm- and Gd-isotopes including the new values for $^{152}$Gd. The maximum for the product of $B(E2)$-values lies between N=88 and N=90 and it does not exactly coincide with the location of the maximum of the $E0$ strength. This may be traced back to the approximation of the Q-phonon scheme applied.

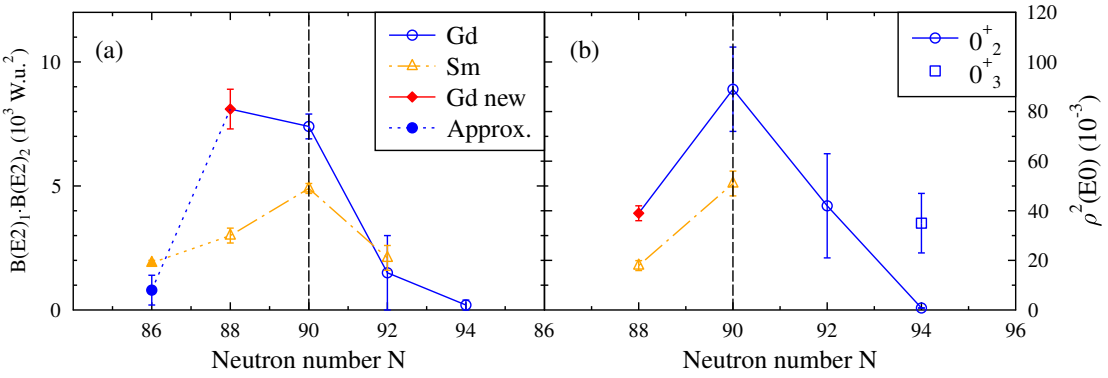


**Figure 5.** (a) Product $B(E2)_1B(E2)_2$ of Gd- and Sm-isotopes. Red (filled diamond) value from [13]. For N=86 isotopes, there is no lifetime data of the $0^+_2$ state. Product $B(E2)_1B(E2)_2$ was approximated as $2 \cdot B(E2)^2$. (b) Experimental values of $\rho^2(E0)$ values for the $0^+_2 \rightarrow 0^+_1$-transition for Gd- (blue) and Sm- (orange) isotopes. Red (filled diamond) value from [13]. For $^{158}$Gd the $\rho^2(E0; 0^+_3 \rightarrow 0^+_1)$ value is shown, too. Note the difference to Figure 1 for $N = 88$.

## 5. Summary

The lifetime of the $0^+_2$ state of $^{152}$Gd was measured using the fast-timing technique. The lifetime of the $0^+_2$ state, 96(6) ps [13] is nearly two times the previously measured value of 53(12) ps [20]. With the new value for $\tau(0^+_2)$ of $^{152}$Gd the $\rho^2(E0)$-transition strength were determined to $39(3)\cdot10^{-3}$ and the $B(E2; 0^+_2 \rightarrow 2^+_1)$-transition strength to 0.536(33) $e^2$b$^2$ or 111(7) W.u.
The $\rho^2(E0)$ values for the $0^+_2$ state and the absolute strength product of the $E2$-$E2$ cascade, $B(E2)_2B(E2)_1$ peak at N=90 or between N=88 and N=90 for the Sm- and the Gd-isotopic chains, respectively indicating the presence of a quantum shape phase transition.

## Acknowledgments

The authors thank the Bucharest Tandem accelerator crew for their support during the experiment. This work was supported by the Deutsche Forschungsgemeinschaft under the Grant No. SFB 634 and the BMBF under the grants 05P15RDFN1/05P15RDFN9 within the collaboration 05P15 NuSTAR R&D.

## References

[1] F. Iachello, Phys. Rev. Lett. **87**, 052502 (2001).
[2] R. F. Casten and N. V. Zamfir, Phys. Rev. Lett. **87**, 052503 (2001).
[3] R. Krücken *et al.*, Phys. Rev. Lett. **88**, 232501 (2002).
[4] P. von Brentano *et al.*, Phys. Rev. Lett. **93**, 152502 (2004).
[5] N. Pietralla and O. M. Gorbachenko, Phys. Rev. C **70**, 0113042 (2004).
[6] J. Bonnet *et al.*, Phys. Rev. C **79**, 034307 (2009).
[7] Nuclear Data Sheets, http://www.nndc.bnl.gov/ensdf.
[8] J. L. Wood *et al.*, Nucl. Phys. A **651**, 323 (1999).
[9] T. Kibédi and R. H. Spear, At. Data Nucl. Data Tables **89**, 77 (2005).
[10] R. F. Casten, Prog. Part. Nucl. Phys. **62**, 183 (2009).
[11] P. Cejnar and J. Jolie, Prog. Part. Nucl. Phys. **62**, 210 (2009).
[12] E. A. McCutchan, N. V. Zamfir and R. F. Casten, Phys. Rev. C **69**, 064306 (2004).
[13] J. Wiederhold *et al.*, Phys. Rev. C **94**, 044302 (2016).
[14] G. Siems *et al.*, Phys. Lett. B **320**, 1 (1994).
[15] T. Otsuka and K.-H. Kim, Phys. Rev. C **50**, R1768 (1994).
[16] N. Pietralla *et al.*, Phys. Rev. Lett. **73**, 2962 (1994).

[17] N. Pietralla *et al.*, Phys. Lett. B **349**, 1 (1995).
[18] N. Pietralla *et al.*, Phys. Rev. C **57**, 150 (1998).
[19] Y. V. Palchikov, P. von Brentano and R. V. Jolos, Phys. Rev. C **57**, 3026 (1998).
[20] N. R. Johnson *et al.*, Phys. Rev. C **26**, 1004 (1982).
[21] D. Bucurescu *et al.*, Nucl. Instrum. Methods Phys. Res. A **837**, 1 (2016).
[22] H. Mach, R. L. Gill and M. Moszyński, Nucl. Instrum. Methods Phys. Res. A **280**, 49 (1989).
[23] M. Moszyński H. Mach, Nucl. Instrum. Methods Phys. Res. A **277**, 407 (1989).
[24] J.-M. Régis *et al.*, Nucl. Instrum. Methods Phys. Res. A **726**, 191 (2013).
[25] N. Marginean *et al.*, Eur. Phys. J. A **46**, 329 (2010).
[26] L. Boström *et al.*, Nucl. Instrum. Methods. **44**, 61 (1966).
[27] V. Werner *et al.*, Phys. Rev. C **93** 034323 (2016).
[28] Z. Bay, Phys. Rev. **77**, 419 (1950).
[29] T. Kíbedi *et al.*, Nucl. Instrum. Methods. Phys. Res. A **589**, 202 (2008).
[30] J. O. Rasmussen, Nucl. Phys. **19**, 85 (1960).